

of the ideal perovskite lattice. This is reflected in the anisotropy of the normal and superconducting state. Various parameters of the normal and superconducting state and in particular the electrical resistance and the critical field H_{C2} show a considerable anisotropy. In addition, the resistance in the ab plane is metallic in contrast to the c -direction where it is of the semiconducting type. The anisotropy of the H_{C2} is usually treated within the Ginsburg-Landau theory with anisotropic parameters ξ, λ, χ . The anisotropy parameter is defined as $\epsilon = \lambda_{\perp}/\lambda_{\parallel}$, where the subscripts refer to the perpendicular and parallel orientation of the magnetic field with respect to the conducting planes. The ratio of the fields H_{C1} is typically between 5 and 10 and about 10 for H_{C2} . Most authors believe that χ lies between 30 and 200 which makes these materials superconductors of the second kind.

Hall effect measurements indicate that the relatively low hole density (about 10^{21} cm^{-3}) carries the normal state current in most of the stoichiometric materials. Critical superconducting currents are typically of the order of 105 A/cm^2 in monocrystals and $103\text{-}104 \text{ A/cm}^2$ in polycrystalline samples. A small isotope effect has been observed in these materials. To study this effect, a well controlled substitution of isotopes is required at the given positions in the crystal lattice. High-quality samples with a small-width of the superconducting transition are, however, lacking and this question is not yet completely elucidated.

In fact it is very difficult to synthesize monocrystals of quality that would satisfy in all respects the high resolution of modern experimental methods and analysis of the data. The reasons lie in the poor knowledge of phase diagrams, incongruity of melting, high toxicity of some chemical components (e.g. thallium complexes), high sensitivity to the profile of cooling, choice of the pots for synthesis etc.

Here, we describe the results of synthesis of high- T_c $\text{Bi}_2\text{Sr}_2\text{CaCuO}_{8-x}$ (BISCO 2212) superconductors (members of the bismuth series $\text{Bi}_2\text{Sr}_2\text{Ca}_{m-1}\text{Cu}_{2m}\text{O}_{4+2m}$ with $m = 2$), obtained by several standard methods. The results of this work should not be considered as final answer to the problem of synthesizing the ideal BISCO monocrystal, but rather as a set of experimental results that indicate how some particular parameters influence the properties of the grown crystals.

For the synthesis of monocrystals $\text{Bi}_2\text{Sr}_2\text{CaCu}_2\text{O}_8$, the following methods have been used: "flux", "self-flux" and "sealed cavity" method. Several syntheses of BISCO monocrystals have been carried out. Some of them were performed in the standard alumina pots, one in a platinum pot whereas in two cases copper pots obtained by electrolysis were used. The latter method has not yet been described in the literature.

2. Description of the apparatus for synthesis of BISCO monocrystals

The experimental set-up consists of the furnace that was specially constructed for the purpose, and of the temperature controlling device. The furnace for the crystal synthesis is shown in Fig. 1. Its principal part is the ceramic element (denoted (r) in Fig. 1) in the form of a hollow cylinder with the internal diameter equal

to 55 mm and the height of 150 mm, wound with the primary heater of Kanthal wire and which contains the vessel where the crystallization takes place. The wire of the heater is wound so as to keep the bottom of the element hotter than the top. On the top, there is an aperture for access to the interior, whereas a small hole at the bottom serves for introducing the holder of the vessel (k). The secondary heater (s), which surrounds the element, is used for modulating the temperature within the furnace. The whole system is imbedded in insulating powder (q) and surrounded by an asbestos layer (o). All of that is placed in the cylindrical metallic container (l), 210 mm high, on which the electric contacts of both heaters are

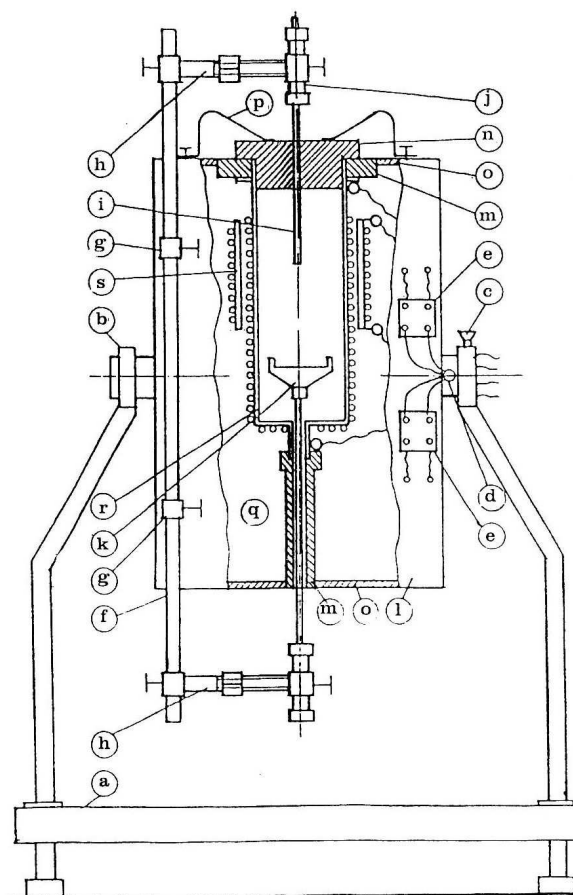


Fig. 1. Furnace for the crystal synthesis: a – support; b – bearing; c – screw; d – hole for wiring for heaters; e – heater connections; f – rod holding the rig holders; g – rig holders; h – holder of accessories; i – bar of mullite; j – bar-of-mullite holder; k – holder of the vessel; l – metallic container; m – ceramic fixture; n – ceramic lid; o – asbestos; p – lid holders; q – insulating powder; r – ceramic element with the heater; s – external ceramic element with the secondary heater element.

positioned (d and e). The element is fixed to the container by ceramic supports for better insulation. The element is covered by a lid (n) which has the holes for the thermocouple and accessories and the lid is fixed by stainless steel clamps. The supports of the rig, which holds the vessel, are fixed on the container. The rig consists of a long metallic rod (f), which is fixed on sleeve contacts parallel to the axis of the furnace, and the holders for fixing the accessories (h) such as the pedestal of the recipient. The holders are constructed so as to allow their positioning along the axis of the furnace, allowing displacement of the vessel along the axis. All this is held by bearings (b) to the support (a). The bearings allow operation in various positions: vertically, upside-down, horizontally or under a given angle. There is a screw (c) on one of the bearings for fixing of the furnace in a desired position. The vessel for crystallization is positioned on the ceramic support (k) which has the form of a saucer, and is placed on a bar of mullite (i) fixed to the holder (j). For better stability, the vessel can be covered by the same kind of holder and held down from above. The way of introducing the vessel into the furnace depends on the method used.

The furnace can reach the temperature of 1010 °C, and the temperature profile of the furnace in the vertical position is such that the temperature decreases from the bottom towards the top, being higher on the cylinder periphery close to the heaters.

The diagram of the device which controls the temperature is given in Fig. 2. It consists of a power amplifier with a DC supply, a Pt-Pt +13% Rh thermocouple, a digital voltmeter (Keithley 193 or 197), a KEPCO 8N-122 programmable D/A converter and of a PC which communicates with instruments via an IEEE 488 communication card.

The process of the temperature stabilization occurs in the following way: the desired temperature is converted into the corresponding voltage using the D/A converter and PC. That voltage is fed to the differential amplifier where it is compared with the voltage from the thermocouple. Their difference regulates the transmissivity of the power transistor, which determines the current in the furnace heater.

The temperature is controlled by a computer program. This program allows for working with a temperature ramp (heating up to a desired temperature and stabilization of this temperature), or for a continuous cooling at the rate of 0.5 to 15 °C/h, or for saw-like profile of cooling at different speeds. The cooling is realized so that on expiration of every (variable) interval of time the controlling voltage i.e. the stabilizing temperature, is diminished by 0.25 °C, and in the meantime the furnace is stabilized at this temperature as in the case of the normal functioning with a temperature ramp. The time rate of decreasing the temperature is controlled by the internal clock of the PC. The temperature stability achieved is ± 1 °C. The saw-like cooling is obtained as a combination of the continuous cooling and temperature stabilization.

The display on the PC shows at any moment the values of the temperature in the furnace, which can be, if desired, stored on the hard disk. Also shown are the data about the desired temperature, control voltage, cooling speed, and the duration of the synthesis.

3. Experimental procedure

3.1. Preparation of the materials for synthesis

The required quantities of very pure Bi_2O_3 , SrCO_3 , CaCO_3 and CuO are weighted in stoichiometric cationic ratio 2:2:1:2

The powders are placed in the ball mill, soaked with petrol-ether and ground for about ten minutes. Petrol-ether ensures good adhesion of the powder to the mill ball, i.e. good grinding and mixing. This liquid is very convenient because it evaporates quickly, resulting in a dry powder.

The so-obtained black powder is pressed into tablets under a pressure of about 2 t/cm^2 , and they can be made even more compact by adding a small quantity (a drop or two) of cyclohexane with 10% of paraffin. The mass of each tablet is about 1.5 g.

The tablets are then inserted into the furnace ("Ney" high-temperature furnace with a thermostat) where they are calcinated in air for 12–15 hours at the temperature of 825°C .

The calcinated tablets are again ground in the way described above and pressed again into tablets and are sintered in air at 850°C . In the course of the sintering, a chemical reaction takes place in the solid state of the mixed ingredients which gives the desired stoichiometric compound. The sintered tablets are ground again, and the powder obtained in this way is ready for the synthesis of the monocrystals.

In some methods, a different initial ratio Bi:Sr:Ca:Cu has been used, as will be pointed out later.

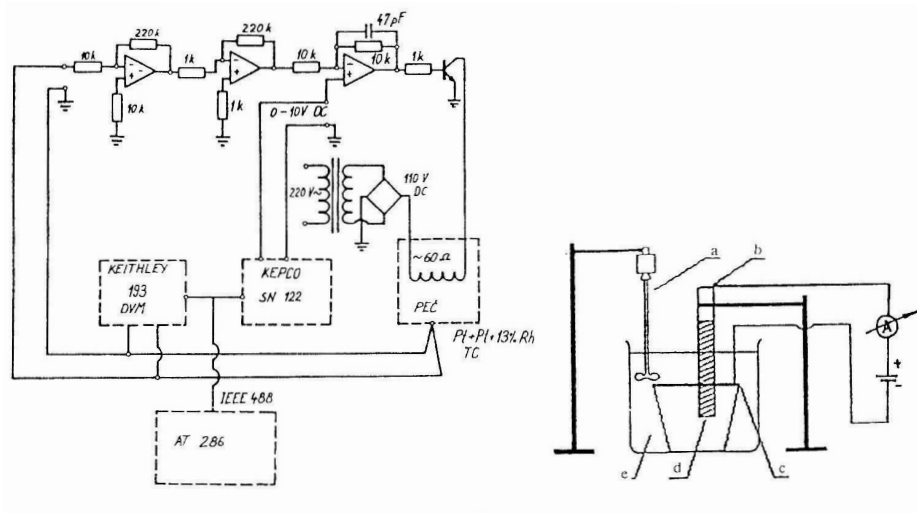


Fig. 2. Diagram of the temperature controller.

Fig. 3. Arrangement for making copper pots by electrolysis (right).

3.2. Production of copper pots by electrolysis

Copper pots for synthesis of BISCO were produced by electrolysis (Fig. 3). The anode (b) is a copper rod, wrapped in glass cloth (d) which prevents contamination of the electrolyte by small particles of copper. A layer of graphite which serves as a cathode, is spread uniformly over the mould of silicon rubber. On the top, in contact with graphite is a copper ring connected to a wire leading to the current supply.

The electrolyte is prepared by dissolving 195–240 g of $\text{CuSO}_4 \times 5 \text{H}_2\text{O}$ in one liter of water and adding subsequently 45–60 g of H_2SO_4 . It is important to carry out this procedure in the described order, because if the acid and water were mixed first, the $\text{CuSO}_4 \times 5 \text{H}_2\text{O}$ would not dissolve, due to the oversaturation of the mixture with SO_4^{2-} ions. In order to get the composition of the electrolyte as homogenous as possible, the electrolyte is slowly agitated with a small propeller on a glass stick (a), driven by a small electric motor at a rate of about three cycles per second. The current density required for the electrolysis is 130–300 A/m^2 .

The electrolysis takes 2–3 days, depending on the thickness of the pot. During this time, the electrolyte can get contaminated by dust, or by small crystals of $\text{CuSO}_4 \times 5 \text{H}_2\text{O}$ (blue vitriol). It is, therefore, recommendable to replace it from time to time by a fresh one, prepared in the same way as described above.

After 2–3 days, the graphite layer is covered by a 1–2 mm thick layer of copper, which is then removed from the mould and the pot thus obtained is ready for use.

3.3. Flux method

Given amounts of Bi_2O_3 , SrCO_3 , CaCO_3 and CuO are taken in the cationic ratio 1:1:1:2, because this stoichiometric relation gives good results. Then KCl is added, which serves as the solvent, so that it makes 80% of the weight of the entire mixture. The ground powder is placed on the bottom of the pot with the salt over it. The pot is covered and placed into the furnace. Such configuration implies the crystal growth on the top of the solution. The solvent dissolves the powder at the hot bottom of the pot and transports it by convection to the colder top, where the crystals are formed.

Platinum pots were used for this synthesis, because attempts to use the alumina have not produced good results. The so obtained crystals are of medium size (1–2 mm), and rather regular in shape. However, the loss of the material is considerable, because of slow transport of the sinterate from the bottom to the top of the melt. Most of the sinterate remains molten at the bottom of the pot and only a small fraction of it crystallizes on the surface. The temperature profile which gave the best crystals is shown in Table 1.

The results of the resistance measurements on a sample obtained by the flux method are shown in Fig. 4.

The measurements are hindered to some extent by relatively large noise due to the high contact resistances (about 200 Ω). The metallic behaviour is observed from room-temperature down to the superconducting transition. The resistance

disappears at 84 K. In the range of temperature 105–110 K, an anomaly in the form of a step was found. This can be ascribed to the presence of the 2223 phase. The amount of this phase is small, and can be firmly identified only using the magnetoresistance measurements, which are very sensitive to the presence of the 2223 phase.

TABLE 1.
The flux method; 1 : 1 : 1 : 2.

Mode of process	time (h)	temperature (°C)	speed of cooling (°C/h)
accelerated heating	—	—	—
stable temperature	15	850	—
saw-like cooling	24	850–814	1.5
continuous cooling	27	814–760	2
continuous cooling	16	760–680	5
continuous cooling	7.5	680–570	15
accelerated cooling	cca 5	570–25	—

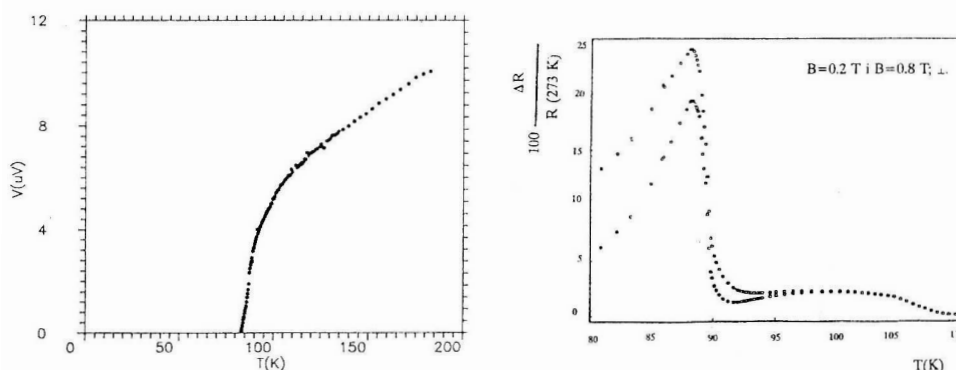


Fig. 4. Plot of resistance vs. temperature of a sample made by the flux method.

Fig. 5. Plot of magnetoresistance vs. temperature for perpendicular fields (right).

Indeed, the measurements in magnetic fields of 0.8 T perpendicular to the ab planes (see Fig. 5) indicate that the samples contains, besides the 2212 phase with $T_c = 88$ K, also the 2223 phase with $T_c = 106$ K. Up to 88 K, the magnetic field increases the dissipation in the superconducting phase. From 88 K to approximately 92 K, the magnetic field acts predominantly on the superconducting fluctuations of the 2212 phase. Above 92 K, the dominant effect is that of the magnetic field on the superconducting state of the 2223 phase.

The measurements of the magnetoresistance in the magnetic field parallel to the ab planes lead to qualitatively the same conclusion, as the measurements with the magnetic field perpendicular to the planes. The measured plots of the resistance vs. temperature also show that the maximum is displaced to lower temperatures

with the increasing field. The dependence of the magnetoresistance on the angle between the field and the c -axis at a given temperature, in the fields between 0.2 and 0.8 T, leads us to the conclusion that the crystal has two sets of ab planes with the angle between them of about 5 °C.

3.4. Self-flux method in Al_2O_3 pot: Cationic ratio 2:2:1.2:2.6

It is known from the literature that the mentioned ratio of cations in the initial mixture leads to very large, high quality 2212 crystals. The excess of copper and calcium should improve the quality of those crystals [3]. Two syntheses have been carried out under exactly the same conditions, in the same pot, using the same temperature profile, the same preparation of the material and with the same ratio of the cations Bi:Sr:Ca:Cu=2:2:1.2:2.6. The temperature profile is given in Table 2.

TABLE 2.
The self-flux method; alumina; 2 : 2 : 1.2 : 2.6; synthesis 2.

Mode of process	time (h)	temperature (°C)	speed of cooling (°C/h)
accelerated heating	—	—	—
stable temperature	12	920	—
continuous cooling	10	920–900	2
continuous cooling	15	900–885	1
continuous cooling	70	885–850	0.5
continuous cooling	45	850–805	1
accelerated cooling	cca 6	805–25	—

The as-prepared crystals are very large (up to 2 mm × 4 mm and several microns thick). They grow in groups inside the small cavities within the solidified melt. They are relatively weakly bound. The crystals are easily cleaved with the surface which is relatively smooth and can be conveniently used for transport measurements.

The chosen cationic ratio decreases the sensitivity of the result on the cooling profile.

The resistance from the room temperature down to the superconducting transition is shown in Fig. 6. In this whole range the resistance is linear with temperature. The scales used in Fig. 6 do not allow to see the step behaviour of the resistance at 106 K. It is shown in Fig. 7. The step is small with respect to the total resistance, what indicates that the amount of the 2223 phase is small. The existence of this phase is confirmed by the magnetoresistance measurements.

The resistance plot in the magnetic fields parallel to the c -axis between 0.2 and 0.8 T and the differential resistance $R(B, T) - R(0, T)$, derived from resistance curve, are shown in Fig. 8.

The second sample from the same series shows a behaviour similar to the first one. The conductivity in the normal state is metallic and there is a step in the resistance at 106 K. This critical temperature is between 87 and 88 K. The state

with $R = 0$ is achieved at approximately 85 K. The step anomaly is present between 105 and 110 K.

We conclude that the excess of copper in the stoichiometric ratio results in metallic conductivity, but leads to a certain amount of the 2223 phase.

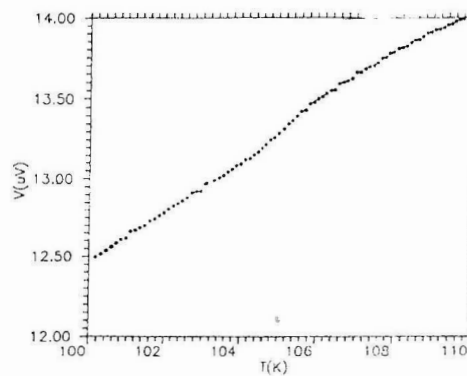
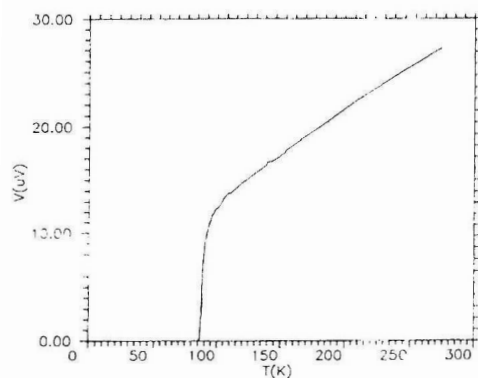


Fig. 6. Plot of resistance vs. temperature of a sample made by the self-flux method in Al_2O_3 pot with cationic ratio 2:2:1.2:2.6.

Fig. 7. Step behaviour of resistance at 106 K of the sample made by the self-flux method in Al_2O_3 pot with cationic ratio 2:2:1.2:2.6 (right).

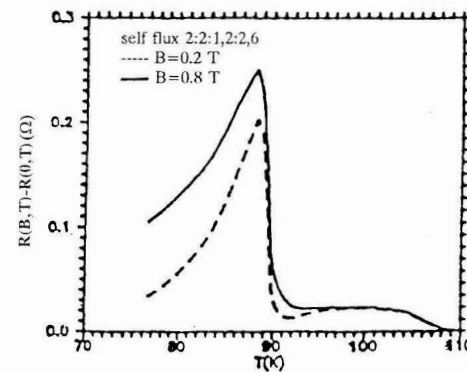
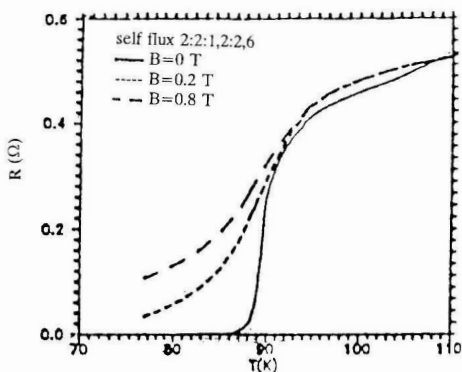


Fig. 8. Plots of resistance vs. temperature in magnetic fields parallel to the c -axis (left), and of differential resistance $R(H, T) - R(0, T)$ (right).

3.5. Self-flux method in Al_2O_3 pot: Cationic ratio 2:2:1:2

Two syntheses were carried out that differ in the temperature profiles. The first profile is described in Table 3. The grown crystals are small, of low quality and there very few of them. This is a consequence of a too fast cooling in the vicinity of

the melting point of $\text{Bi}_2\text{Sr}_2\text{CaCu}_2\text{O}_8$ (875°C). In an attempt to avoid the freezing-in of the crystallographic defects, it is incorrect to impose a slow cooling below the melting temperature. Small, dirty and irregular resulting surface of the crystal makes it inadequate for measuring the transport properties. For this reason they have not been performed.

The second synthesis used the temperature profile described in Table 4, whereas the other parameters were kept the same. The as grown crystals have the surface at about $1\text{ mm} \times 3\text{ mm}$ and are several microns thick. The crystals amass within the small cavities. A large number of crystals in the form of small needles and thin ribbons were observed. Their composition was not determined.

TABLE 3.
The self-flux method; alumina; 2 : 2 : 1 : 2; synthesis 1.

Mode of process	time (h)	temperature ($^\circ\text{C}$)	speed of cooling ($^\circ\text{C}/\text{h}$)
accelerated heating	—	—	—
stable temperature	20	920	—
continuous cooling	5.5	920–900	3.5
continuous cooling	60	900–870	0.5
continuous cooling	35	870–800	2
continuous cooling	48	800–560	5
accelerated cooling	cca 5	560–25	—

TABLE 4.
The self-flux method; alumina; 2 : 2 : 1 : 2; synthesis 2.

Mode of process	time (h)	temperature ($^\circ\text{C}$)	speed of cooling ($^\circ\text{C}/\text{h}$)
accelerated heating	—	—	—
stable temperature	20	905	—
continuous cooling	10	905–895	1
continuous cooling	120	895–835	0.5
continuous cooling	30	835–805	1
continuous cooling	7.5	805–790	2
accelerated cooling	cca 6	790–25	—

In both syntheses the alumina pots were strongly eroded due to a reaction of the melt with the alumina. They could not be reused.

The resistance plots of the samples in this series are shown in Figs. 9 and 10. These samples show the metallic conductivity down to 150 K, at which point the resistance starts to increase on lowering the temperature towards the superconducting transition at 95 K. Such behaviour does not affect the critical temperature which is only 1 K lower than that found in the samples described in Section 3.4, and corresponds to the critical temperature of the 2212 phase.

Measuring the resistance of several samples allowed to reject the possibility that the upturn in the resistance was caused by a contribution along the c -axis.

The resistance is of the order of magnitude of what is usually found for the *ab* planes and is smaller than that in the *c*-direction.

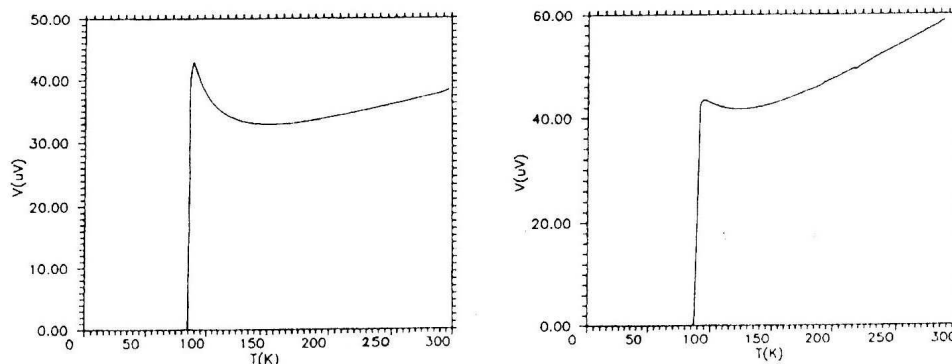


Fig. 9. Plot of resistance vs. temperature of a sample made by the self-flux method in Al_2O_3 pot with cationic ratio 2:2:1:2.

Fig. 10. Plot of resistance vs. temperature of the second sample made by the self-flux method in Al_2O_3 pot with cationic ratio 2:2:1:2 (right).

The resistance plot does not show the anomaly in the temperature range 100–120 K, which is expected in crystals with a certain amount of the 2223 phase. We conclude that the initial stoichiometric ratio of cations leads to the crystals free of the 2223 phase but with the upturn in resistance between 150 and 95 K.

3.6. Sealed cavity method

Appropriate amounts of Bi_2O_3 , SrCO_3 , CaCO_3 and CuO are taken in cationic ratio 1:1:1:2 and 0:1:1:4. The mixture 0114 is calcinated a 930°C in air for 40 hours and is sintered at 980°C also in air for 12 hours.

Following the method described in Ref. 4, the small lumps of 1112 are first placed into the pot, and over them are placed the lumps of the 0114 compound. The closed pot is then placed into the furnace. The commercial furnace ELPH-2 was used with the built-in microprocessor which controls the temperature profile. The profile is described in Table 5.

The syntheses were carried out by this method, one in alumina and the other in a copper pot. The temperature profile and other parameters were the same in both syntheses. In order to protect the furnace, the copper pot was also placed into an alumina pot, which turned out to be justified because a strong reaction between the melt and the copper resulted in the dissolving of the copper pot.

It was expected that 1112 could be doped by 0114 with Sr, Ca, Cu, preventing evaporation of Bi from 1112 and that a sealed cavity could be formed in which the crystals of $\text{Bi}_2\text{Sr}_2\text{CaCu}_2\text{O}$ could grow.

The results obtained did not justify these expectations. The mentioned cavity

has not formed, but rather, everything got mixed into a mass without crystals of the well-known $\text{Bi}_2\text{Sr}_2\text{CaCu}_2\text{O}_8$ layered morphology. If such crystals do form locally, their small dimensions and strong bonding to the solidified melt makes their use for transport measurements impossible.

TABLE 5.
The sealed cavity method.

Mode of process	time (h)	temperature ($^{\circ}\text{C}$)	speed of cooling ($^{\circ}\text{C}/\text{h}$)
accelerated heating	—	—	—
stable temperature	20	905	—
continuous cooling	10	905–895	1
continuous cooling	120	895–835	0.5
continuous cooling	30	835–805	1
accelerated cooling	—	—	—

4. Conclusion

The results of syntheses and measurements described in this work indicate that the production of high-quality monocrystals of BISCO 2212 is a considerable problem, which limits understanding of the detailed properties of its normal and superconducting state. In particular, mixing of the two phases, $\text{Bi}_2\text{Sr}_2\text{CaCu}_2\text{O}_8$ with $T_c = 85$ K and $\text{Bi}_2\text{Sr}_2\text{CaCu}_2\text{O}_{10}$ with $T_c = 110$ K is the problem which has not yet been successfully solved.

It is clear that the alumina pots are subject to erosion and that this exposes the crystals to contamination. It is planned to use pots of materials which better resist erosion by the melt. The synthesis of the crystals in the copper pots was attempted here for the first time. The quality of the grown crystals depends very much on the method and the parameters of the synthesis. The monocrystals entirely free of the 2223 phase have not been obtained.

The measurements of the resistance show the superconducting transition with the (mean) temperature of 88 K, whereas the resistance falls to zero at 85.5 K. The magnetoresistance measurements exhibit clearly the presence of the $\text{Bi}_2\text{Sr}_2\text{CaCu}_2\text{O}_{10}$ phase with the transient temperature of about 106 K. The magnetoresistance in the superconducting state shows an anisotropy with respect to the orientation of the magnetic field with the largest contribution for the parallel and the smallest contribution for the perpendicular orientation with respect to the c -axis of the crystal.

In the range of a few kelvins below T_c , the behaviour of the magnetoresistance agrees well with the prediction of the superconducting fluctuation theory. The resistance curve in the absence of the magnetic field shows a step in the range 105–110 K.

In the case of a very small amount of the second phase, this step may be completely absent, i.e., the contribution of this phase can be entirely masked. In the measurements of the magnetoresistance in strong magnetic fields, this contribution

can then be misinterpreted as the fluctuative contribution to the conductivity above T_c of BISCO 2212.

In further work we will seek methods of producing the monocrystals which will contain a smaller amount of the 2223 phase.

Acknowledgement

The author is grateful to Prof. B. Leontić and Mr. D. Babić for their collaboration and help in this work.

References

- 1) L. F. Schneemeyer, R. B. von Dover, S. H. Glavium, S. A. Sunshine, R. M. Fleming, B. Batlogg, T. Siegrist, I. H. Morshall, I. V. Waszczak and L. W. Rupp, *Nature* **332** (1988) 422;
- 2) W. L. McMillan, *Phys. Rev.* **167** (1968) 331;
- 3) P. D. Han and D. A. Payne, *J. Crystal Growth* **104** (1990) 201;
- 4) S. J. Guo et al., *J. Crystal Growth* **100** (1990) 303.

SINTEZA MONOKRISTALA BISCO (2212) I MJERENJA NEKIH NJIHOVIH TRANSPORTNIH SVOJSTAVA

Opisana je oprema i metoda rasta monokristala BISCO (2212) i to metoda "fluksa" (Flux-method), dvije metode "vlastitog fluksa" (self-flux) te metoda "zatvorene šupljine" (sealed cavity). Sve metode izuzev posljednje pokazale su se uspješnima u određenom opsegu. Ipak, još uvijek nije realiziran monokristal u potpuno čistoj fazi 2212. Postotak faze 2223 vrlo je malen i za većinu transportnih mjerenja nezamjetljiv. Tijekom rada stečeno je iskustvo koje ukazuje na uvjete sinteza kojima će se ostvariti rast čiste faze 2212.